

2013

Characterization of spindle-E: a protein involved in guarding the genome

<https://hdl.handle.net/2144/12177>

"Downloaded from OpenBU. Boston University's institutional repository."

BOSTON UNIVERSITY
SCHOOL OF MEDICINE

Thesis

**CHARACTERIZATION OF SPINDLE-E: A PROTEIN INVOLVED IN
GUARDING THE GENOME**

by

KRISTEN OTT

B.S., Bay Path College, 2008

Submitted in partial fulfillment of the
requirements for the degree of
Master of Arts

2013

Approved by

First Reader

Caryn Navarro, Ph.D.
Assistant Professor of Medicine

Second Reader

Kim McCall, Ph.D.
Associate Professor of Biology

CHARACTERIZATION OF SPINDLE-E: A PROTEIN INVOLVED IN GUARDING THE GENOME

KRISTEN OTT

Boston University School of Medicine, 2013

Major Professor: Caryn Navarro, Ph.D., Assistant Professor of Medicine

ABSTRACT

Transposable selfish genetic elements (TSE) account for a large percentage of the human genome, as well as the genomes of most other organisms. When active, TSEs can transpose (excise and insert) within the genome. Dysregulation of TSEs results in accumulation of DNA double strand breaks, a high rate of mutation, chromosomal rearrangements, and sterility. Silencing of TSEs in the germline has been attributed to a specialized class of small, non-coding RNAs, named Piwi-interacting RNA (piRNA). *Drosophila spindle-E (spnE)* has been identified as a central component of the piRNA pathway. SpnE is conserved and is necessary for the generation of most ovarian piRNAs in *Drosophila* and mouse. Both the SpnE and mouse TDRD9 proteins contain a DExH box helicase domain and a Tudor domain and are required for TE silencing and germline development. Through the analysis of several new mutant *spnE* alleles, we show that the highly conserved DExH box helicase region is required for proper piRNA pathway function. We also show that mutations in the helicase region lead to the

formation of Dynein motor complex aggregates as well as the mislocalization of the piRNA binding protein Aubergine (Aub).

TABLE OF CONTENTS

| | |
|--|------|
| Title | i |
| Reader's Approval Page | ii |
| Abstract | iii |
| Table of Contents | v |
| List of Tables | vii |
| List of Figures | viii |
| List of Abbreviations | ix |
| Introduction | 1 |
| Methods | 6 |
| Drosophila Strains | 6 |
| Induction of germline clones | 6 |
| Sequencing | 6 |
| Antibody production | 7 |
| Protein isolation and Western blot analysis | 8 |
| D/V patterning assay | 8 |
| Real time PCR | 9 |
| Immunohistochemistry and microscopy | 10 |
| Results | 12 |
| Expression of mutant protein | 12 |
| Dorsal-ventral patterning defects in mutants | 18 |

| | |
|---|----|
| DEXH Box mutations disrupt piRNA pathway function | 21 |
| DEXH Box mutations cause Dynein aggregates | 25 |
| DEXH Box mutations affect Aubergine localization | 26 |
| Discussion | 32 |
| List of Journal Abbreviations | 35 |
| References | 36 |
| Curriculum Vitae | 40 |

LIST OF TABLES

| Table | Name | Page |
|-------|---|------|
| 1 | <i>spnE</i> mutant alleles show differing phenotypes | 13 |
| 2 | Many <i>spnE</i> mutant alleles have defects in DV patterning | 19 |

LIST OF FIGURES

| Figure | Title | Page |
|--------|---|------|
| 1 | <i>spnE</i> alleles express mutant protein | 16 |
| 2 | Retrotransposon levels are upregulated in <i>spnE</i> mutants | 23 |
| 3 | Formation of Dynein aggregates in <i>spnE</i> mutant ovaries | 27 |
| 4 | Aub nuage localization in <i>spnE</i> mutant ovaries | 30 |

ABBREVIATIONS

| | |
|--------------|-------------------------------------|
| DNA | Deoxyribonucleic acid |
| DV | Dorsal/Ventral |
| EMS | ethyl methanesulfonate |
| miRNA | micro RNA |
| piRNA | Piwi-interacting RNA |
| RNA | ribonucleic acid |
| sDMA | symmetrically dimethylated arginine |
| siRNA | small interfering RNA |
| TGF α | Transforming Growth Factor α |
| TSE | Transposable selfish element |

Introduction

Transposable selfish elements and the piRNA pathway Transposable selfish genetic elements (TSEs) are abundant in eukaryotic genomes. There are different classes of TSEs, some of which are present in high copy numbers throughout the genome. When active, TSEs can excise and insert within the genome. Active TSEs cause damage to the host genome by creating an abundance of DNA double strand breaks, insertion mutations, and chromosome rearrangements. In the germline this leads to the passing of damaged DNA from parent to offspring which then leads to developmental defects or sterility.

TSE silencing in animal germlines is attributed to a class of small, non-coding RNAs called Piwi-interacting RNA (piRNA)[1, 2]. piRNAs were discovered in the *Drosophila* germline and have subsequently been identified in *C. elegans*, mouse, and humans. piRNAs are 24-28 nucleotide RNAs that bind to specific members of the Argonaute protein family in order to form a silencing complex for retrotransposons. piRNAs differ from other, more well-known classes of regulatory RNAs such as miRNAs and siRNAs. Most importantly, they are generated independent of Dicer activity[1, 2].

piRNA biogenesis begins with the HP1 homolog Rhino and the DNA binding protein Cutoff localizing to distinct piRNA clusters located in pericentromeric and sub-telomeric heterochromatic regions[3]. Transcription from these regions creates a long, single-stranded RNA precursor. The precursor RNA is then processed into shorter primary piRNAs through an unknown

mechanism. In *Drosophila*, different populations of piRNAs are found in the germ cells and the ovarian soma[4]. Somatic piRNA biogenesis is complete after primary piRNAs are processed. Somatic piRNA biogenesis is known to involve the piRNA binding protein Piwi, the Tudor domain protein Yb, and the RNA helicase Armitage[5, 6]. In germ cells, the primary piRNAs enter into the ping-pong amplification loop to increase the pool of available piRNAs and create an adaptive response[1, 2, 7]. Aubergine (Aub) and Argonaute 3 (Ago3) are two piRNA binding proteins known to be directly involved in the amplification process[8]. Aub binds anti-sense piRNAs and Ago3 binds sense piRNAs. Amplification begins when Aub binds an anti-sense primary piRNA. The Aub-piRNA complex is then guided to a sense transcript of an active transposon or the sense transcript from a piRNA cluster. Aub, which possesses slicer activity, cleaves the sense transcript and loads it onto Ago3. Ago3 is then guided to a complementary anti-sense RNA, probably derived from the piRNA cluster, which it cleaves and loads onto Aub. The amplification loops allows an adaptive response to the presence of active transposon mRNA.

In addition to the Argonaute proteins (Piwi, Aub, and Ago3), many proteins have been identified as playing a role in the germline piRNA pathway, by affecting biogenesis, amplification, or both. These proteins generally localize to the cytoplasm directly surrounding the nucleus known as the nuage[9]. These proteins include the RNA-binding protein Vasa, nucleases Squash and Zucchini, and Tudor-domain containing proteins Krimper and Tejas[10-13]. While

mutations in these genes interrupt piRNA pathway function, their exact roles within the pathway remain unknown.

Drosophila oogenesis *Drosophila* oogenesis begins with the division of a germline stem cell to produce a renewed stem cell as well as a cystoblast. The cystoblast continues to divide until it becomes a 16 cell cyst. The cells do not divide completely, leaving cytoplasmic bridges connecting the cells to one another. Two cells within the cyst will have four connections to other cells. One of these cells will be designated as the oocyte and the other 15 cells will become nurse cells[14]. The oocyte undergoes meiotic arrest and accumulates factors necessary for growth and development while the nurse cells undergo endoreplication and transport the factors that are important for oocyte growth and development. As the oocyte matures, specialized RNAs become localized to specific locations within the oocyte to ensure proper embryonic patterning. For example, *gurken* (*grk*) RNA, a TGF α -like molecule, is localized to the dorsal anterior corner of the oocyte in order to induce proper dorsal/ventral patterning[15].

Oogenesis defects in piRNA pathway mutants piRNA pathway mutant females exhibit many defects in oogenesis as well as a decrease in piRNA levels leading to the upregulation of retrotransposons. In the early stages of oogenesis, an increased accumulation of DNA double strand breaks can be observed[16-18]. This may be due to an increase in transposon activity, but this has not been confirmed. piRNA mutant females also show decreased levels of Grk protein in

the later stages of oogenesis. The decrease in Grk causes dorsal/ventral (D/V) patterning defects in the eggs laid by piRNA mutant females[11, 16, 17]. Another phenotype that is characteristic of mutations in the piRNA pathway is the formation of Dynein aggregates within the egg chamber. These aggregates are thought to be caused by microtubule defects and may function as sites of retrotransposon RNA degradation[19].

In most piRNA pathway mutants, the D/V patterning defects, as well as Dynein aggregation and microtubule network defects, are due to the activation of a DNA damage checkpoint governed by the Chk2 (Checkpoint kinase 2) protein kinase[16-19]. However how checkpoint activation leads to these defects is currently unknown.

Spindle-E in the piRNA pathway Among proteins that localize to the nuage, Spindle-E (SpnE) has been identified as a central component of the piRNA pathway in germ cells. Previous work has shown that mutations in *spnE* cause a global downregulation of germline piRNAs[4]. In contrast, most other piRNA pathway mutations affect the levels of only a subset of piRNAs. Checkpoint activation does not seem to be responsible for the D/V patterning defects of *spnE* mutants. The failure of *chk2* mutations to suppress the eggshell phenotype in *spnE* mutants is just one way in which *spnE* mutants differ from other piRNA pathway mutants. *spnE* mutant females also lay a high percentage of collapsed eggs while other piRNA pathway mutants do not. The differences between the

spnE mutant phenotypes and other piRNA pathway mutant phenotypes indicate that SpnE may be playing multiple roles throughout oogenesis.

SpnE has three conserved domains: a DExH box RNA helicase domain, a Tudor domain, and a Zinc finger domain. DExH box helicase domains are known to be involved in splicing, translation initiation, as well as other aspects of RNA metabolism. Tudor domains have been shown to specifically bind to symmetrically dimethylated arginines and are abundant in proteins expressed in the *Drosophila* ovary. Zinc fingers are most commonly found in DNA binding proteins, however because SpnE localizes to the cytoplasm, it is more likely that it would be involved in RNA binding or mediating protein-protein interactions. Both the DExH box helicase and Tudor domain are highly conserved in SpnE's mammalian homolog, TDRD9. Here, we show that SpnE's DExH box helicase domain is required for proper piRNA pathway function.

Materials and Methods

Drosophila strains

The following *Drosophila* lines were used: $w;FRT[ry^+]82BspnE^{4-48}e$, $w;FRT[ry^+]82BspnE^{66-21}e$, $w;FRT[ry^+]82BspnE^{100-37}e$, $w;FRT[ry^+]82BspnE^{189-39}e$, $w;FRT[ry^+]82BspnE^{114-33}e$, $w;FRT[ry^+]82BspnE^{155-55}e$, and $w;FRT[ry^+]82BspnE^{23-17}e$ were a kind gift from R. Lehmann and described in [34]. $yw;FRT[ry^+]82BspnE^{2A9-14}$, $yw;FRT[ry^+]82BspnE^{9A2-17}$, $yw;FRT[ry^+]82BspnE^{9A9-18}$, $yw;FRT[ry^+]82BspnE^{8D4-11}$, $yw;FRT[ry^+]82BspnE^{4E2-14}$, and $yw;FRT[ry^+]82BspnE^{7G2-5}$ were a kind gift from D. St. Johnston and described in [20]. $spnE^{\Delta 125}$ was a kind gift from C. Berg and described in [21]. The wild-type strain used was Oregon-R.

Induction of germline clones

Germline clones were induced using the FLP/FRT system [22]. $FRT82BspnE$ females were crossed to $ywhsflp(ii);FRT82BubiGFP$ male flies (Bloomington stock center). Second or third instar larvae were heat shocked at 37°C for two hours on two consecutive days to induce clones.

Sequencing

Genomic DNA was isolated as in [23]. 30 adult male flies were homogenized in 400µl of Buffer A (100mM Tris pH 7.5, 100mM EDTA, 100mM NaCl, and 0.5% SDS) and incubated at 65°C for 30 minutes. 800µl of Buffer B (1 part 5M KAc:

2.5 parts 6M LiCl) was added and the lysate was centrifuged at 15,000rpm at room temperature for 15 minutes. 1 mL of the supernatant was transferred to a new tube and 600 µl of isopropanol was added to precipitate the DNA. The precipitate was centrifuged for 15 minutes to pellet the DNA. The pellet was washed with 70% ethanol, allowed to air dry, and resuspended in 150µl of Tris-EDTA. Sections of the *spnE* gene were amplified from 1µl of the genomic DNA prep using standard PCR conditions and Crimson Taq (New England Biosystems). Multiple sets of *spnE* gene-specific primers that span the gene from the start codon to the stop codon, including introns were used. PCR products were purified using Qiagen's MinElute PCR purification kit. Sanger sequencing was done by the Molecular Genetics Core Facility at Boston University School of Medicine.

Spindle-E and Aubergine antibody production

Rabbit polyclonal antisera directed against peptide MNLPPNPVIARGRGRG (amino acids 1-16) [7] of Aub and TNHRRKHSIGKFYRDQLG (amino acids 295-312) of SpnE was generated by Pocono Rabbit Farm and Laboratory, Inc. using their Quick Draw 49 Day protocol. The antisera was affinity purified by Pocono Rabbit Farms using the appropriate peptide.

Protein isolation and Western blot analysis

2-3 day old female flies were fattened overnight on yeast and ovaries were dissected in 1x EBR (130mM NaCl, 4.7mM KCl, 1.9mM CaCl₂, and 10mM Hepes pH 6.9). Ovaries were homogenized 5-10 times in lysis buffer (50 mM Tris-HCl pH 8.0, 150 mM NaCl, 1% NP40, 1x Halt protease inhibitor single-use cocktail [Thermo Scientific]). Samples were centrifuged twice for 5 minutes at 12,000g at 4°C to remove nuclei. Protein was quantitated using a Biorad Protein Assay. 40µg of protein were resolved on 7% SDS-polyacrylamide gels and transferred to PVDF membranes (Immobilon) using the Bio-Rad mini-PROTEAN tetra electrophoresis system. Western blots were done as in [23]. Primary antibodies were diluted at 1:1000 in 5% non-fat milk in Tris-buffered saline with 0.5% Tween. Antibodies used were mouse anti-β-tubulin (Developmental Studies Hybridoma Bank) and affinity purified rabbit anti-Spindle-E. HRP-conjugated secondary antibodies (Jackson ImmunoResearch Laboratories) were used at a dilution of 1:10,000. For detection, the blots were incubated in, Amersham ECL Prime Western Blotting Detection Reagent (GE Healthcare) according to the manufacturer's instructions and exposed to x-ray film (Kodak Biomax light or Amersham). Bands were quantitated using NIH ImageJ software.

D/V Patterning Assay

2-3 day old female flies of the specified genotypes were fattened on yeast overnight, placed into condos, and allowed to lay eggs on apple juice agar plates

with yeast paste overnight at 25°C. Eggs of each class were counted after 24 hours of egg laying for three consecutive days.

Real Time PCR

2-3 day old female flies were fattened overnight on yeast. Ovaries were dissected in EBR and placed in eppendorf tubes. The EBR was removed and the ovaries were flash frozen in liquid nitrogen or used fresh for RNA isolation. RNA was isolated using TRIzol reagent (Invitrogen) according to the manufacturer's instructions. RNA was treated with Turbo DNase (Ambion) two times to remove contaminating genomic DNA. cDNA was generated from 1µg of RNA using the Verso cDNA kit (Thermo Scientific) or the Maxima cDNA kit (Fermentas). A 10µl real time PCR reaction was performed with either 1x ABsolute blue Sybrgreen master mix (Abgene), 0.075 mM of forward and reverse primers, and 1µl of cDNA reaction OR 1x Maxima Sybr master mix (Fermentas), 0.3 mM of forward and reverse primers, and 1µl of cDNA reaction. Cycling parameters were: 50 °C, 2 min; 95 °C, 10 min; 95 °C, 15 sec; 60 °C, 1 min for 40 cycles using an ABI 7900HT. The following previously published primers were used: HetA: 5'-ATCCTTCACCGTCATCACCTTCCT-3', 5'-GGTGCGTTTAGGTGAGTGTGTGTT-3', TART: 5'-ATTCCTGCCTGGTTAGATCGCAA-3', 5'-AGAGAGGGAAAGAAGGGAAAGGGA-3', I-Factor: 5'-GACCAAATAAAAATAATACGACTT-3', 5'-AACTAATTGCTGGCTTGTTATG-3',

Blood: 5'-AACAAATAGAAAGAAGCCACCGAAC-3', 5'-
AGTCATGGACTATTGAGGGTGTTG-3' Roo: 5'-
CGTCTGCAATGTACTGGCTCT-3', 5'-CGGCACTCCACTAATTCTCC-3', Adh:
5'-CCGTGGTCAACTTCACCAGCTC-3', 5'-
TCCAACCAGGAGTTGAACGTGTGC-3'. Data were analyzed using SDS
software.

Immunohistochemistry and microscopy

Ovaries from 2-3 day old fattened females were dissected in 1x EBR and fixed in 200µl 2% formaldehyde and 0.5% NP40 in PBS plus 600µl heptane for 20 minutes. Following fixation, ovaries were rinsed 3 times in PBST (PBS + 0.2% Tween) then washed three times for five minutes each in PBST. Ovary membranes were permeabilized by incubating with 1% Triton-X in PBST for 1 hour. Ovaries were then blocked with 1% BSA and 2% donkey serum in PBST for 1 hour, then incubated with primary antibody overnight at 4°C. Chicken anti-GFP (Abcam) was used at a dilution of 1:5000, rabbit anti-Egalitarian was used at a dilution of 1:5000 [23], and rabbit anti-Aubergine was used at a dilution of 1:1000. Following primary antibody incubation, ovaries were washed three times for 20 minutes each in PBST, re-blocked for 1 hour, then incubated for 2 hours with secondary antibodies (Cy3- Jackson ImmunoResearch, Alexa488- Molecular Probes) at a concentration of 1:500 in PBST containing 1% BSA. Ovaries were washed 3 times for 20 minutes in PBST, incubated with DAPI (1:1000) for 10

minutes, and washed a final time before mounting onto slides in 50% PBS, 50% glycerol, and 2.5% 1,4-diazabicyclo[2.2.2]octane (Sigma Aldrich). Images were captured using a Zeiss 510 LSM confocal microscope and processed using ImageJ and/or Photoshop software.

Results

Several mutant lines contain point mutations in the *spnE* coding region:

To begin our analysis of the conserved domains of Spindle-E, 12 *spnE* mutant lines from two independent EMS mutagenesis screens were collected (**Table 1**). Six mutant alleles were isolated in a screen to identify genes that affected anterior posterior axis specification and the other six in a screen for dorsal ventral patterning defects [20, 34]. Through mapping and complementation testing, these mutant lines were identified as *spnE* mutants, but were not further characterized. To begin our characterization of the 12 mutant alleles, each was crossed with *spnE*^{hlsΔ125}, a deficiency in the *spnE* region [24]. The resulting *spnE* hemizygous ovaries were examined for SpnE protein expression via Western Blot. We determined that eight of the alleles expressed SpnE protein at the same molecular weight as wild type SpnE protein (**Fig 1C**). The levels of SpnE protein produced by the point mutations were compared to levels detected from wild type ovarian extracts and heterozygous *spnE* mutant extracts (**Fig 1D**). Hemizygous mutants were used as they express lower levels of SpnE protein as compared to wild type, yet do not have a mutant phenotype. The eight protein producing alleles were then sequenced to determine the nature and location of the mutation.

TABLE 1 *spnE* mutant alleles show differing phenotypes

| Allele | Protein | Mutation | Affected domain | DV patterning defects | Retrotransposon expression | Dynein Aggregate Formation | Aub nuage localization |
|---------------------|---------|------------|-----------------|-----------------------|----------------------------|----------------------------|------------------------|
| 2A9-14 ¹ | + | Thr145Ile | DExH Box (I) | severe | ↑↑↑ | + | - |
| 7G2-5 ¹ | + | Thr233Ile | DExH Box (I/II) | severe | ↑↑↑ | + | - |
| 155-55 ² | + | Glu239Lys | DExH Box (II) | severe | ↑↑↑ | + | - |
| 23-17 ² | + | His241Gln | DExH Box (II) | mild | ↑ | - | +/- |
| 8D4-11 ¹ | + | Ser435Phe | DExH Box (V) | severe | ↑↑↑ | + | - |
| 9A2-17 ¹ | + | Pro508Leu | btwn domains | mild | ↑↑ | | + |
| 4-48 ² | + | Glu717Lys | btwn domains | mild | ↑ | - | + |
| 66-21 ² | + | His1422Leu | Zinc Finger | mild | ↑ | - | + |
| 100-37 ² | - | ND | | severe | ↑↑↑ | + | - |
| 114-33 ² | - | ND | | severe | ↑↑↑ | + | - |
| 9A9-18 ¹ | - | ND | | severe | ↑↑↑ | + | - |
| 4E2-14 ¹ | - | ND | | severe | ↑↑↑ | + | - |

Table 1 Ovarian phenotypes were characterized for each allele. Number in parentheses next to DExH box corresponds to conserved motif. Severe DV patterning defects indicate that the majority of the eggs laid were collapsed, whereas mild indicates a majority of wild type eggs. ↑↑↑ indicates all retrotransposons tested were upregulated. ↑ indicates only some retrotransposons were upregulated. (+) indicates presence of Dynein aggregates were present and Aub localization to the nuage. (-) indicates absence of aggregates, Aub not localized to nuage. +/- represents partial Aub localization to the nuage. ND- not determined

¹ Mutant alleles identified from [20]

² Mutant alleles identified from an EMS screen in the Lehmann lab [34]

Five alleles were found to have point mutations in the DExH Box helicase domain, one allele had a point mutation in the zinc finger, and two mutations were found between the conserved domains (**Fig 1A**). It has been shown that the DExH Box helicase domain consists of several conserved regions, each playing a specific role in the unwinding of nucleic acids. Previously, mutations in regions I, II, and V that are similar to the mutations found in the *spnE* alleles were studied in the yeast splicing protein Prp22 and the vaccinia virus protein NPH-I (alignment in **Fig 1B**) [25-29]. Most mutations in the DExH box of Prp22 are lethal. Mutations in the conserved GKT sequence in Reg I and the glutamic acid of Reg II result in a drastic decrease in ATPase activity in both viral and yeast models [25, 28, 29]. However, mutations in the histidine of Reg II still maintain some ATPase activity and are not lethal in yeast. Reg V of the DExH Box has not been as extensively studied as other regions, but has been implicated in RNA binding.

The two mutations (*spnE*⁴⁻⁴⁸ and *spnE*^{9A2-17}) were found to be in residues that were outside of the conserved domains of SpnE, but are conserved between SpnE and the mammalian homolog TDRD9, implying that they may still be required for function. The only mutation that is in a domain not conserved in TDRD9 is the mutation in the zinc finger (*spnE*⁶⁶⁻²¹). A zinc finger domain is only found in *Drosophila* SpnE and the homolog in mosquitos.

Figure 1

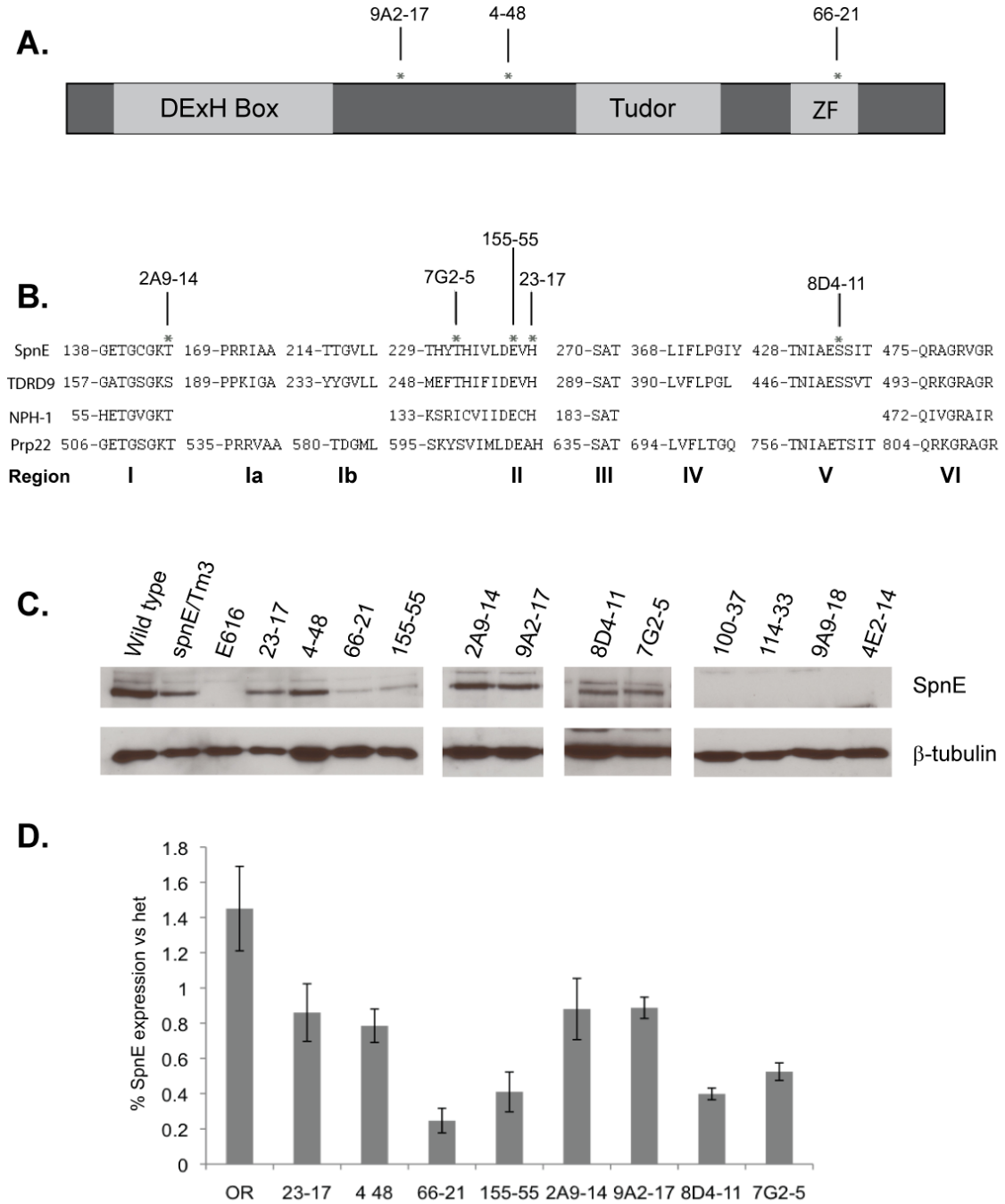


Figure 1 Eight of the twelve *spnE* alleles express detectable protein and have point mutations in the *spnE* coding region. **(A)** Domain structure of SpnE. SpnE contains a highly conserved DExH box and Tudor domains as well as a zinc finger. The position of the two mutations outside of the conserved domains as well as in the zinc finger are shown. **(B)** The amino acid sequence of SpnE's DExH box domain compared to its vertebrate homolog TDRD9 and vaccinia virus protein NPH-I. The position of the five mutations identified in the SpnE DExH box domain are shown. **(C)** SpnE protein expression in mutant ovary extracts was measured by Western. Eight alleles express detectable protein of the correct size for SpnE. Four alleles do not express detectable protein. **(D)** SpnE protein levels in the various mutant ovaries relative to *spnE*^{Δ125}/TM3. Error bars represent standard deviation of 2 separate protein isolates.

Some *spnE* mutations cause dorsal-ventral patterning defects:

Mutations in the piRNA pathway are known to disrupt proper dorsal/ventral patterning through the activation of the Chk2 checkpoint [16-18]. However, the D/V patterning defects seen in *spnE* mutants are not due to Chk2 activity and are typically more severe than other piRNA mutants. Patterning defects are detected by scoring the eggs laid by mutant females for defects in dorsal appendage formation. In wild type eggs, two dorsal appendages are visible on the anterior of the egg. D/V patterning defects cause deformities in dorsal appendage formation resulting in fused appendages or a lack of appendage formation. Severe D/V patterning defects can cause the females to lay empty eggshells, or collapsed eggs.

spnE null mutant females lay a high percentage of eggs that are collapsed, indicative of severe patterning defects (**Table 2**). This phenotype is also seen in eggs laid by females with a DExH Box mutation in *spnE* with the one exception being the mutation affecting the histidine in Reg II of the DExH Box (*spnE*²³⁻¹⁷). As previously described, mutations in this residue tend to be less disruptive to function as compared to other residues. Eggs laid by *spnE*²³⁻¹⁷ mutant females still exhibit mild D/V patterning defects, shown by the presence of eggs lacking dorsal appendages or having one fused dorsal appendage. However, the majority of the eggs laid show a wild type phenotype with two dorsal appendages at the anterior of the egg. The severity of D/V patterning

TABLE 2 Many *spnE* mutant alleles have defects in dorsal ventral patterning

| | Allele | Wild type | Fused | None | Collapsed | Total Eggs |
|--------------|---------|-----------|-----------|----------|-----------|-------------|
| | hls/TM3 | 100% | 0% | 0% | 0% | 600+ |
| DExH box | 2A9-14 | 1% ± <1% | 3% ± 5% | 11% ± 4% | 85% ± 9% | 380 |
| | 7G2-5 | 4% ± 5% | 4% ± 3% | 3% ± 4% | 89% ± 11% | 638 |
| | 155-55 | 6% ± 3% | 12% ± 1% | 18% ± 7% | 64% ± 5% | 742 |
| | 23-17 | 43% ± 9% | 33% ± 4% | 18% ± 7% | 6% ± 2% | 684 |
| | 8D4-11 | 0% ± 0% | 1% ± 2% | 0% ± 0% | 99% ± 2% | 99 |
| btwn domains | 9A2-17 | 61% ± 24% | 36% ± 22% | 3% ± 2% | 0% ± 0% | 771 |
| | 4-48 | 70% ± 10% | 28% ± 9% | 2% ± <1% | 0% ± 0% | 835 |
| Zinc finger | 66-21 | 92% ± 2% | 7% ± 2% | 1% ± 1% | 0% ± 0% | 1129 |
| nulls | 100-37 | 2% ± 3% | 11% ± 4% | 28% ± 4% | 59% ± 12% | 630 |
| | 114-33 | 0% ± 0% | 4% ± <1% | 11% ± 6% | 85% ± 5% | 677 |
| | 9A9-18 | 0% ± 0% | 0% ± 0% | 0% ± 0% | 100% ± 0% | 410 |
| | 4E2-14 | 0% ± 0% | 3% ± 3% | 6% ± 2% | 91% ± 1% | 414 |

Table 2 Dorsal-ventral patterning defects were quantitated by collecting eggs from *spnE* mutant female flies and determining the percentage of eggs with two dorsal appendages (wild type), fused dorsal appendages, no dorsal appendages, and eggs that were collapsed. Calculations are from two separate experiments, each consisting of three 24 hour egg collections.

defects seen in the *spnE* DExH box mutants correlate with viability of Prp22 DExH box mutant yeast.

In contrast, females carrying *spnE* mutations between the conserved domains (*spnE*⁴⁻⁴⁸ and *spnE*^{9A2-17}) and the mutation affecting the zinc finger (*spnE*⁶⁶⁻²¹) lay a high percentage of wild type eggs as well as a higher number of total eggs as compared to females carrying null mutations and mutations in the DExH box. This indicates that mutations in the DExH Box helicase domain of SpnE are as detrimental to oocyte development as the complete loss of SpnE protein.

DExH box helicase mutations disrupt SpnE's function in the piRNA

pathway:

piRNA pathway mutants all have a set of similar phenotypes, including D/V patterning defects, increased expression of retrotransposable elements, and the formation of Dynein motor complex aggregates [4, 16, 19]. To determine the impact of the various *spnE* mutations on the ability of the piRNA pathway to effectively silence retrotransposable elements, we used quantitative real time PCR to determine the RNA levels of five transposable elements in each of the *spnE* mutants.

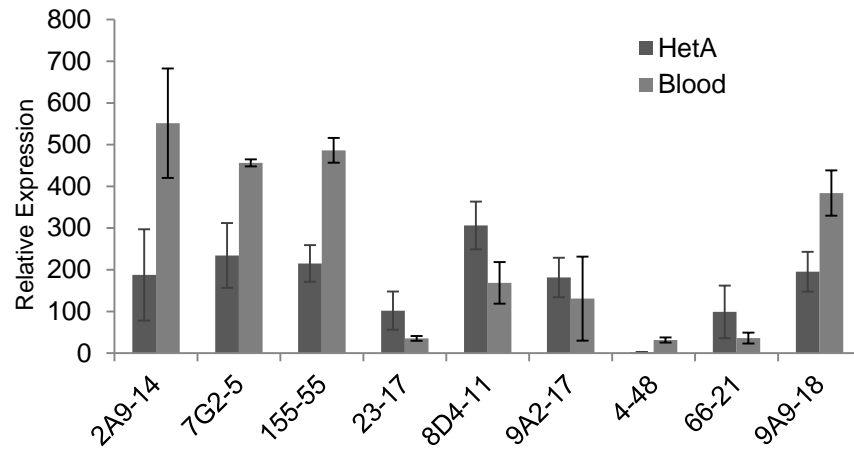
HetA and Blood are two retrotransposons with high copy numbers throughout the genome. In wild type ovaries, HetA is required to replicate and maintain telomeres and Blood is a highly abundant retrotransposon that is

normally silenced by the piRNA pathway. In *spnE* null mutants (represented by *spnE*^{9A9-18} in **Fig 2**), HetA RNA levels increase approximately 200 fold and Blood increases approximately 350 fold as compared to their heterozygous siblings (**Fig 2A**). The DExH Box mutations *spnE*^{2A9-14}, *spnE*^{7G2-5}, *spnE*¹⁵⁵⁻⁵⁵, and *spnE*^{8D4-11}, all of which caused severe D/V patterning defects, had similar upregulation of both HetA and Blood. The mutation in the histidine of Reg II of the DExH Box (*spnE*²³⁻¹⁷) and the mutation in the zinc finger (*spnE*⁶⁶⁻²¹) showed upregulation of the HetA and Blood, but not as severe as the *spnE* null mutant. Interestingly, the two mutations between the conserved domains gave differing phenotypes. *spnE*^{9A2-17} mutants had HetA expression levels similar to null mutants, however Blood levels were significantly lower than that of the null mutants. *spnE*⁴⁻⁴⁸ was the only mutant to show no significant upregulation of HetA, Blood, or any of the other transposons examined.

I Factor, TART, and roo are three transposons with lower copy numbers that tend to not become as highly expressed in piRNA pathway mutants as compared to HetA and Blood. I Factor, a LINE retrotransposon, and roo, a non-LTR retrotransposon, are normally repressed by the piRNA pathway. TART is another transposable element that is necessary for telomere maintenance, but will become overexpressed in the absence of a functioning piRNA pathway. *spnE* null mutant ovaries show increases of approximately 15 fold of I Factor RNA, 30 fold for TART RNA, and 5 fold for roo RNA (**Fig 2B**). As seen with HetA and

Figure 2

A.



B.

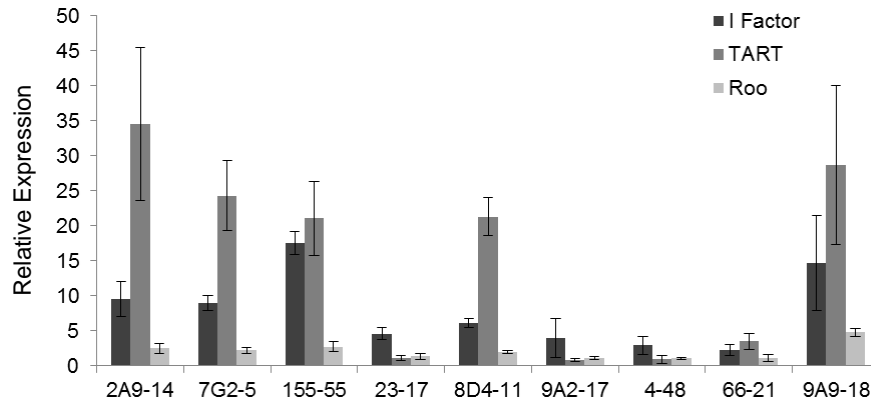


Figure 2 Retrotransposon RNA levels are increased to varying degrees in the various *spnE* mutant ovaries. **(A)** real time PCR for the retrotransposons Het-A and Blood using extracts from mutant ovaries. **(B)** real time PCR for retrotransposons I Factor, TART, and roo. All *spnE* mutant RNAs were normalized to their heterozygous siblings. Error bars represent standard deviation of four experiments using two independent RNA isolates.

Blood, four of the five DExH Box alleles had expression levels similar to the *spnE* null phenotype, whereas *spnE*²³⁻¹⁷, *spnE*⁶⁶⁻²¹, *spnE*⁴⁻⁴⁸ all have expression levels significantly lower than the nulls. However, *spnE*^{9A2-17} has minimal upregulation of all three retrotransposons differing from the expression levels of HetA and Blood. This could indicate that some mutations in *spnE* can affect only a subset of retrotransposons or that transposons with high copy numbers are more sensitive to disruptions to the piRNA pathway.

Mutations in the DExH Box cause the formation of Dynein aggregates

Previous work has shown that activation of the Chk2 checkpoint caused by a mutation in the piRNA pathway causes several phenotypes in the *Drosophila* ovary [17]. One such phenotype is the formation of Dynein aggregates within the egg chamber. These aggregates have been shown to contain members of the Dynein motor complex, patterning RNA, and retrotransposon RNA [19]. This aggregation of proteins inhibits the proper transport of patterning RNAs which then causes defects in the patterning of the eggs. If the aggregates are disrupted the levels of retrotransposon RNA increases, and they are therefore thought to be sites of retrotransposon degradation.

To determine which *spnE* mutations would cause the formation of Dynein aggregates, we used the FLP-FRT system to create germline clones of each mutant and used immunohistochemistry to compare wild type egg chambers with

the homozygous mutant chambers. An α -GFP antibody was used to differentiate wild type and mutant egg chambers. Presence of GFP indicates a wild type egg chamber whereas the absence of GFP indicates a homozygous mutant egg chamber (**Fig 3 A-E**). To detect the presence or absence of Dynein aggregates, an α -Egalitarian (Egl) antibody was used (**Fig 3 A'-E'**). Egl is an adapter that binds to Dynein in order to load cargo onto the complex. In wild type egg chambers, Egl localizes strongly to the oocyte, which is the most posterior cell in the egg chamber (**Fig 3 A''**). Egl localized to the oocyte only, with no aggregate formation in *spnE*⁴⁻⁴⁸ (**Fig 3 B''**), *spnE*²³⁻¹⁷ (**Fig 3 C''**), *spnE*^{9A2-17}, and *spnE*⁶⁶⁻²¹. The remainder of the *spnE* mutant egg chambers, including *spnE*¹⁵⁵⁻⁵⁵ (**Fig 3D''**) and *spnE*^{9A9-18} (**Fig 3E''**), contained Dynein aggregates. Because Dynein aggregates have been shown to be an effect of Chk2 activation, this could mean that DExH Box mutations in SpnE are severe enough to activate the checkpoint, whereas mutations to the Zinc finger domain and between the conserved domains are not as detrimental and do not activate the checkpoint, allowing proper microtubule function and therefore D/V patterning to occur.

Some *spnE* mutations affect localization of the piRNA pathway protein

Aubergine:

piRNA proteins are recruited to the nuage in a specific order [9, 13]. It has been shown that mutations in one piRNA pathway protein can affect the localization of one or more other members of the pathway to the nuage [12]. We

Figure 3

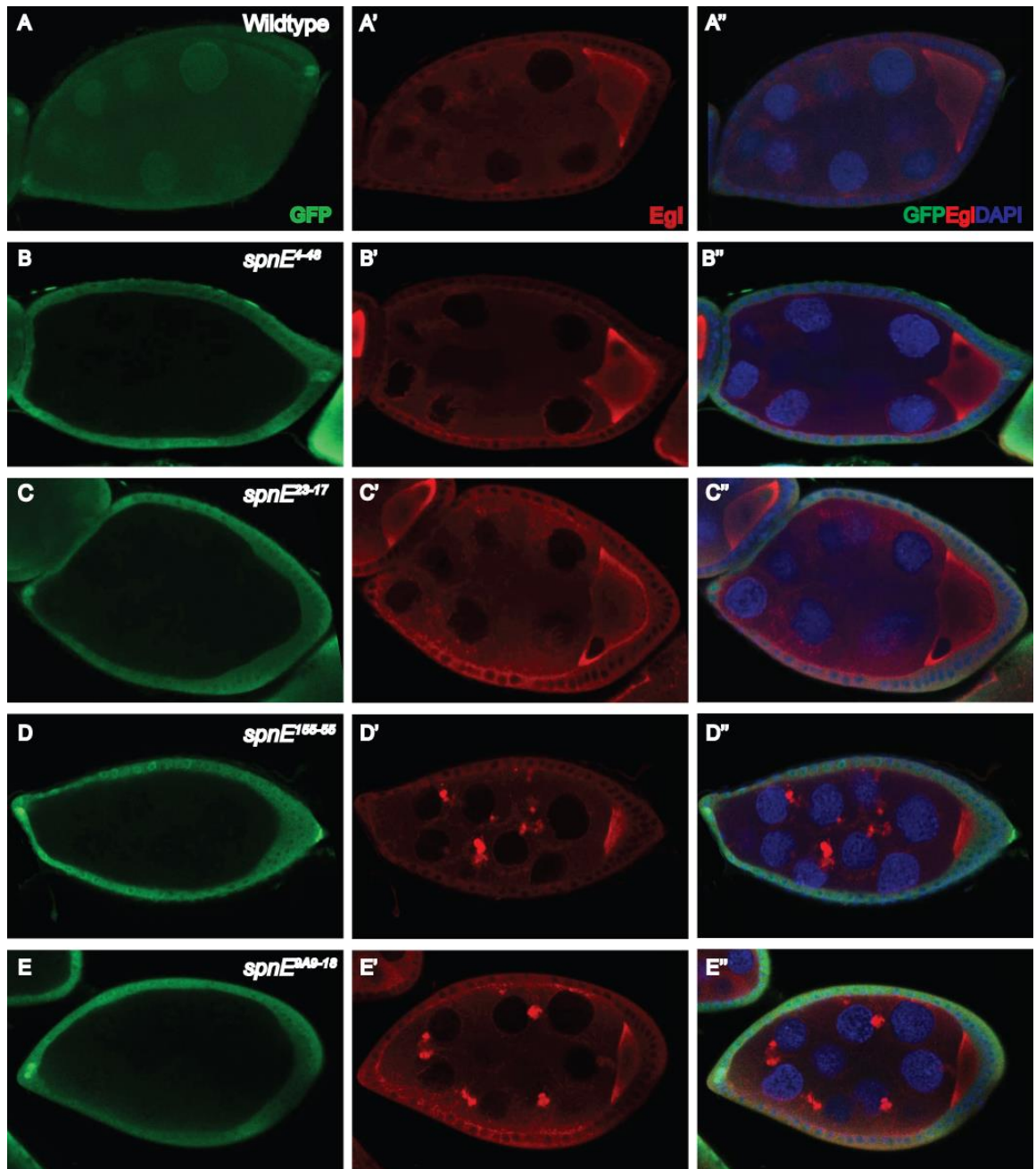


Figure 3 Dynein motor complex aggregates form in some, but not all *spnE* mutant ovaries. *spnE* mutant germline clones are marked by the absence of GFP. All egg chambers are stained with α -GFP (green) to mark clones, α -Egalitarian (Egl) (red), and the DNA dye DAPI. In wild type egg chambers, Egl is dispersed throughout the nurse cells and localizes to the oocyte (**A-A''**). *spnE*⁴⁻⁴⁸ (**B-B''**), *spnE*²³⁻¹⁷ (**C-C''**), as well as *spnE*^{9A2-17} and *spnE*⁶⁶⁻²¹ (not shown) show wild type Egl localization. In *spnE*^{9A9-18} null egg chambers (**E-E''**) Egl forms aggregates throughout the egg chamber. This phenotype is present in *spnE*¹⁵⁵⁻⁵⁵ mutant egg chambers (**D-D''**) as well as *spnE*^{2A9-14}, *spnE*^{7G2-5}, *spnE*^{8D4-11}, and the remainder of the null alleles (not shown).

used an α -Aub antibody to examine the expression and localization of Aub protein in stage 4/5 egg chambers of each *spnE* mutant. Again, we utilized the FLP-FRT recombination system to create germline clones in order to compare Aub localization in wild type and mutant chambers side by side. In wild type egg chambers, Aub localizes to the nuage, the cytoplasm directly surrounding the nurse cell nuclei (**Fig 4 A''**). In *spnE*⁴⁻⁴⁸ (**Fig 4 B''**), *spnE*^{9A2-17}, and *spnE*⁶⁶⁻²¹ mutant egg chambers, Aub is localized to the nuage and resembles the wild type egg chambers present in their respective ovarioles. In *spnE*²³⁻¹⁷, which has shown phenotypes similar to the previously characterized *spnE* alleles, we see an intermediate phenotype where Aub protein is expressed, but is punctate (**Fig C''**). Aub is still localizing to the nuage, but the expression levels at the nuage are diminished as compared to the wild type egg chambers above and to the right of the mutant chamber (outlined in white) (**Fig C'**). The remainder of the *spnE* alleles, including the DExH box mutant *spnE*¹⁵⁵⁻⁵⁵ (**Fig D'**, white outline) and the null *spnE*^{9A9-18} (**Fig E'**, white outline) do not have Aub localization to the nuage. It also appears that these mutations show decreased cytoplasmic levels of Aub as compared to the wild type egg chambers surrounding them. From this we can conclude that SpnE's DExH Box is involved in the localization, and possibly the expression of Aub protein.

Figure 4

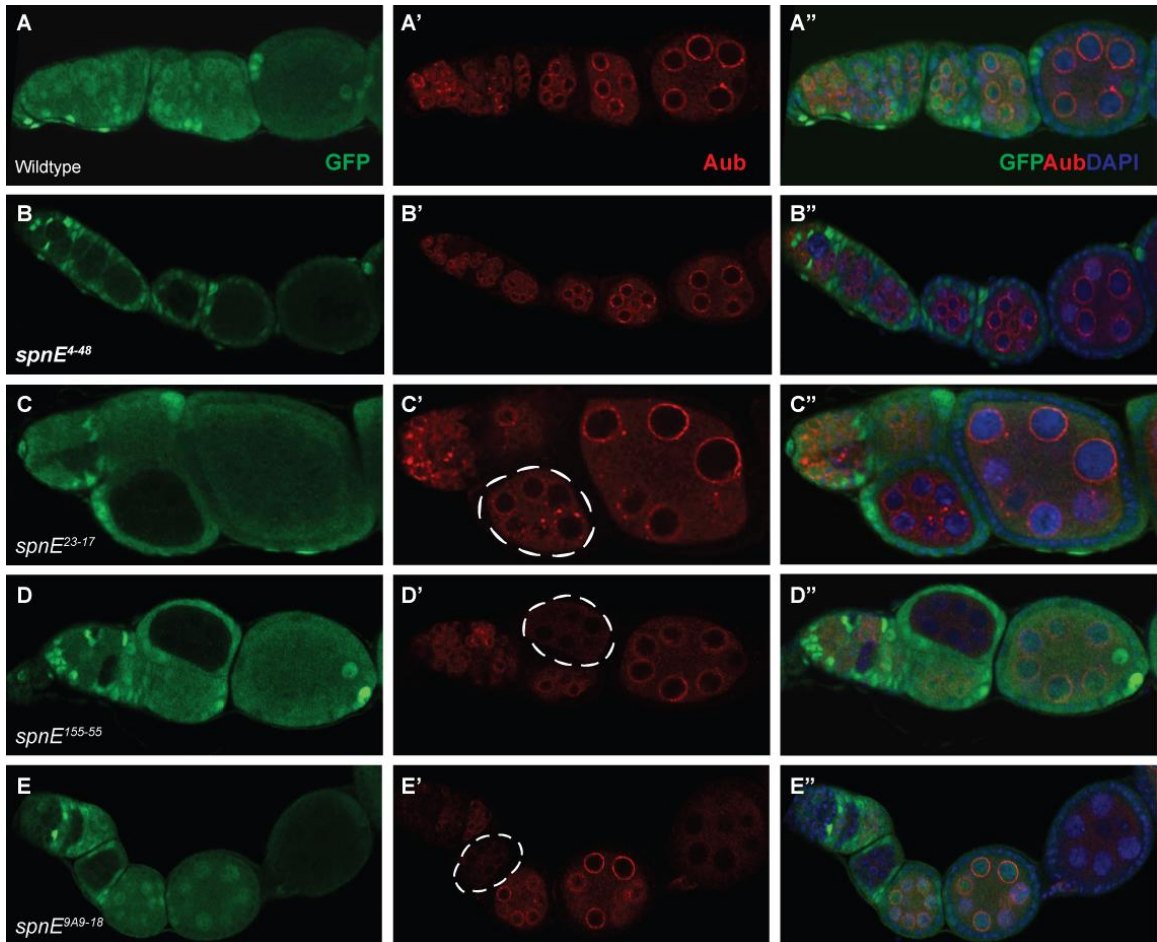


Figure 4 Aub nuage localization is lost in some, but not all of the various *spnE* mutant egg chambers. *spnE* mutant germline clones are marked by the absence of GFP. All egg chambers are stained with α -GFP (green), α -Aub (red), and DAPI. In wild type egg chambers Aub localizes to around the nurse cell nuclei to a structure known as the nuage. (**A-A''**). *spnE*⁴⁻⁴⁸ (**B-B''**), *spnE*^{9A2-17}, and *spnE*⁶⁶⁻²¹ (not shown) show wild type localization of Aub to the nuage. *spnE*²³⁻¹⁷ shows an intermediate phenotype where Aub expression is punctate (**C-C''**, egg chamber outlined in **C'**) and only partially localized to the nuage. In *spnE*^{9A9-18} null ovaries (**E-E''**) Aub is not localized to the nuage and levels of Aub protein appear to be decreased in mutant egg chambers (**E'**, outlined). This phenotype is seen in *spnE*¹⁵⁵⁻⁵⁵ mutant egg chambers (**D-D''**) as well as *spnE*^{2A9-14}, *spnE*^{7G2-5}, *spnE*^{8D4-11}, and the remainder of the null alleles (not shown).

Discussion:

Spindle-E and its mammalian homolog TDRD9 have been shown to be an integral part of the piRNA pathway in the germlines of both *Drosophila* and mouse, but not much is known about the molecular function of SpnE. Through this study we have shown that the DExH box helicase domain of SpnE is required for its proper function by characterizing 12 mutant alleles of *spnE* and placing them into two phenotypic categories. The mild *spnE* mutants (*spnE*²³⁻¹⁷, *spnE*⁴⁻⁴⁸, *spnE*⁶⁶⁻²¹, and *spnE*^{9A2-17}) lay a high percentage of wild type eggs, have minimal upregulation of retrotransposons, do not form Dynein aggregates, and have wild type Aub localization. The remainder of the *spnE* mutant alleles, including four of the five DExH Box helicase mutant alleles, are characterized as severe mutants. They lay a high percentage of collapsed eggs, have highly elevated levels of retrotransposon RNA, form Dynein aggregates in their egg chambers, and have mislocalized and/or decreased Aub expression.

With the *spnE* DExH Box mutants and *spnE* null mutants both falling into the severe phenotypic category, it can be inferred that mutations in SpnE's DExH Box effectively disable SpnE from functioning in the germline. The one exception being the mutation to the histidine in Reg II of the DExH Box, which has been shown in yeast to be a milder DExH Box mutation and is not fatal to the yeast.

Interestingly, the mutation in the zinc finger (*spnE*⁶⁶⁻²¹) did not appear to have an impact in SpnE's function. *spnE*⁶⁶⁻²¹ produced the least amount of protein among the alleles we studied, yet did not show any mutant phenotypes.

This verifies that the mutations are the cause of the mutant phenotype and not the decreased level of SpnE protein. Therefore, we can be confident that the mutant phenotypes that we did see are due to the mutation and not to the level of protein that was produced. As mentioned previously, the mammalian homolog of SpnE, TDRD9, does not have a zinc finger domain. This could mean that the Zinc finger domain is not necessary for SpnE's function within the piRNA pathway, but could possibly play another role in *Drosophila* ovaries or early embryos.

We did not find any alleles of *spnE* that had a mutation in the Tudor domain. Analysis of mutations in the Tudor domain would help give insight into binding partners of SpnE, as Tudor domains are known to bind exclusively to other proteins that have symmetrically dimethylated arginines (sDMAs). Both Tudor domains and proteins with sDMAs are abundant in the piRNA pathway and the germline in general. Therefore, there are many proteins that could form a complex with SpnE. Identifying these proteins and how the Tudor domain interacts with them will help in understanding the molecular function of SpnE within the piRNA pathway.

These data suggest that SpnE's function within the piRNA pathway involves binding to RNA, as DExH Box helicase domains are known to be involved in various parts of RNA metabolism. SpnE could bind directly to pre-piRNAs after they are exported from the nucleus to the nuage, where SpnE could unwind them for processing. There are many proteins that form a complex in the

nuage that is responsible for the processing and modification of piRNAs. It is possible SpnE is part of this complex and assists in piRNA amplification by unwinding piRNAs. We also showed that *spnE* mutants affect the expression and localization of Aub and therefore could be affecting the piRNA pathway indirectly. It's possible that SpnE could be involved in the translation of Aub protein, as we see a decrease in null and DExH box helicase *spnE* mutant egg chambers. While further experiments are needed to fully understand the molecular function of SpnE, we know that the DExH Box helicase domain, but not the zinc finger, is required in order for SpnE to function in its critical role of the piRNA pathway.

Understanding how SpnE/TDRD9 functions within the piRNA pathway will help give us insight into human disease caused by piRNA pathway disruption and aberrant retrotransposon expression. Recently, decreased expression of human TDRD9, PIWI, and TDRD1 were found to cause a complete loss of sperm production in human males [30]. This indicates that mutations in the piRNA pathway may be able to account for previously unidentifiable causes of infertility. Understanding how the piRNA pathway functions may bring us closer to treatments for infertility. In contrast, expression of piRNAs and piRNA pathway proteins outside of the germline has been linked to cancer progression and prognosis [31-33]. This may lead to the use of piRNA pathway proteins as a biomarker for cancer prognosis. Continued study of the piRNA pathway and associated proteins is integral in understanding human development and disease.

Journal Abbreviations

| | |
|--------------------|---|
| Curr Biol | Current Biology |
| Dev Cell | Developmental Cell |
| Genes Dev | Genes & Development |
| J Biol Chem | Journal of Biological Chemistry |
| J Viral | Journal of Virology |
| Nat Cell Bio | Nature Cell Biology |
| Proc Natl Acad Sci | Proceedings of the National Academy of Sciences |
| RNA Biol | RNA Biology |

REFERENCES

1. Aravin, A.A., Hannon, G.J., and Brennecke, J. (2007). The Piwi-piRNA pathway provides an adaptive defense in the transposon arms race. *Science* 318, 761-764.
2. Klattenhoff, C., and Theurkauf, W. (2008). Biogenesis and germline functions of piRNAs. *Development* 135, 3-9.
3. Pane, A., Jiang, P., Zhao, D.Y., Singh, M., and Schupbach, T. (2011). The Cutoff protein regulates piRNA cluster expression and piRNA production in the *Drosophila* germline. *EMBO J* 30, 4601-4615.
4. Malone, C.D., Brennecke, J., Dus, M., Stark, A., McCombie, W.R., Sachidanandam, R., and Hannon, G.J. (2009). Specialized piRNA pathways act in germline and somatic tissues of the *Drosophila* ovary. *Cell* 137, 522-535.
5. Saito, K., Ishizu, H., Komai, M., Kotani, H., Kawamura, Y., Nishida, K.M., Siomi, H., and Siomi, M.C. (2010). Roles for the Yb body components Armitage and Yb in primary piRNA biogenesis in *Drosophila*. *Genes Dev* 24, 2493-2498.
6. Cook, H.A., Koppetsch, B.S., Wu, J., and Theurkauf, W.E. (2004). The *Drosophila* SDE3 homolog armitage is required for oskar mRNA silencing and embryonic axis specification. *Cell* 116, 817-829.
7. Brennecke, J., Aravin, A.A., Stark, A., Dus, M., Kellis, M., Sachidanandam, R., and Hannon, G.J. (2007). Discrete small RNA-generating loci as master regulators of transposon activity in *Drosophila*. *Cell* 128, 1089-1103.
8. Siomi, M.C., and Kuramochi-Miyagawa, S. (2009). RNA silencing in germlines--exquisite collaboration of Argonaute proteins with small RNAs for germline survival. *Current opinion in cell biology* 21, 426-434.
9. Lim, A.K., and Kai, T. (2007). Unique germ-line organelle, nuage, functions to repress selfish genetic elements in *Drosophila melanogaster*. *Proc Natl Acad Sci U S A* 104, 6714-6719.
10. Vagin, V.V., Klenov, M.S., Kalmykova, A.I., Stolyarenko, A.D., Kotelnikov, R.N., and Gvozdev, V.A. (2004). The RNA interference proteins and vasa

locus are involved in the silencing of retrotransposons in the female germline of *Drosophila melanogaster*. *RNA Biol* 1, 54-58.

11. Pane, A., Wehr, K., and Schupbach, T. (2007). *zucchini* and *squash* encode two putative nucleases required for rasiRNA production in the *Drosophila* germline. *Dev Cell* 12, 851-862.
12. Patil, V.S., and Kai, T. (2010). Repression of retroelements in *Drosophila* germline via piRNA pathway by the Tudor domain protein *Tejas*. *Curr Biol* 20, 724-730.
13. Nagao, A., Sato, K., Nishida, K.M., Siomi, H., and Siomi, M.C. (2011). Gender-Specific Hierarchy in Nuage Localization of PIWI-Interacting RNA Factors in *Drosophila*. *Frontiers in genetics* 2, 55.
14. Navarro, C., Lehmann, R., and Morris, J. (2001). Oogenesis: Setting one sister above the rest. *Curr Biol* 11, R162-165.
15. Neuman-Silberberg, F.S., and Schupbach, T. (1993). The *Drosophila* dorsoventral patterning gene *gurken* produces a dorsally localized RNA and encodes a TGF alpha-like protein. *Cell* 75, 165-174.
16. Klattenhoff, C., Bratu, D.P., McGinnis-Schultz, N., Koppetsch, B.S., Cook, H.A., and Theurkauf, W.E. (2007). *Drosophila* rasiRNA pathway mutations disrupt embryonic axis specification through activation of an ATR/Chk2 DNA damage response. *Dev Cell* 12, 45-55.
17. Chen, Y., Pane, A., and Schupbach, T. (2007). *Cutoff* and *aubergine* mutations result in retrotransposon upregulation and checkpoint activation in *Drosophila*. *Curr Biol* 17, 637-642.
18. Abdu, U., Brodsky, M., and Schupbach, T. (2002). Activation of a meiotic checkpoint during *Drosophila* oogenesis regulates the translation of *Gurken* through Chk2/Mnk. *Curr Biol* 12, 1645-1651.
19. Navarro, C., Bullock, S., and Lehmann, R. (2009). Altered dynein-dependent transport in piRNA pathway mutants. *Proc Natl Acad Sci U S A* 106, 9691-9696.
20. Martin, S.G., Leclerc, V., Smith-Litierre, K., and St Johnston, D. (2003). The identification of novel genes required for *Drosophila* anteroposterior axis formation in a germline clone screen using GFP-*Staufen*. *Development* 130, 4201-4215.

21. Gillespie, D.E., and Berg, C.A. (1995). Homeless is required for RNA localization in *Drosophila* oogenesis and encodes a new member of the DE-H family of RNA-dependent ATPases. *Genes Dev* 9, 2495-2508.
22. Harrison, D.A., and Perrimon, N. (1993). Simple and efficient generation of marked clones in *Drosophila*. *Curr Biol* 3, 424-433.
23. Navarro, C., Puthalakath, H., Adams, J.M., Strasser, A., and Lehmann, R. (2004). Egalitarian binds dynein light chain to establish oocyte polarity and maintain oocyte fate. *Nat Cell Biol* 6, 427-435.
24. Gonzalez-Reyes, A., Elliott, H., and St Johnston, D. (1997). Oocyte determination and the origin of polarity in *Drosophila*: the role of the spindle genes. *Development* 124, 4927-4937.
25. Schneider, S., Campodonico, E., and Schwer, B. (2004). Motifs IV and V in the DEAH box splicing factor Prp22 are important for RNA unwinding, and helicase-defective Prp22 mutants are suppressed by Prp8. *J Biol Chem* 279, 8617-8626.
26. Schwer, B., and Gross, C.H. (1998). Prp22, a DExH-box RNA helicase, plays two distinct roles in yeast pre-mRNA splicing. *EMBO J* 17, 2086-2094.
27. Wagner, J.D., Jankowsky, E., Company, M., Pyle, A.M., and Abelson, J.N. (1998). The DEAH-box protein PRP22 is an ATPase that mediates ATP-dependent mRNA release from the spliceosome and unwinds RNA duplexes. *EMBO J* 17, 2926-2937.
28. Deng, L., and Shuman, S. (1998). Vaccinia NPH-I, a DExH-box ATPase, is the energy coupling factor for mRNA transcription termination. *Genes Dev* 12, 538-546.
29. Gross, C.H., and Shuman, S. (1995). Mutational analysis of vaccinia virus nucleoside triphosphate phosphohydrolase II, a DExH box RNA helicase. *J Virol* 69, 4727-4736.
30. Heyn, H., Ferreira, H.J., Bassas, L., Bonache, S., Sayols, S., Sandoval, J., Esteller, M., and Larriba, S. (2012). Epigenetic disruption of the PIWI pathway in human spermatogenic disorders. *PLoS One* 7, e47892.
31. Greither, T., Koser, F., Kappler, M., Bache, M., Lautenschlager, C., Gobel, S., Holzhausen, H.J., Wach, S., Wurl, P., and Taubert, H. (2012).

Expression of human Piwi-like genes is associated with prognosis for soft tissue sarcoma patients. *BMC cancer* 12, 272.

32. Qiao, D., Zeeman, A.M., Deng, W., Looijenga, L.H., and Lin, H. (2002). Molecular characterization of hiwi, a human member of the piwi gene family whose overexpression is correlated to seminomas. *Oncogene* 21, 3988-3999.
33. Wang, Y., Liu, Y., Shen, X., Zhang, X., Chen, X., Yang, C., and Gao, H. (2012). The PIWI protein acts as a predictive marker for human gastric cancer. *International journal of clinical and experimental pathology* 5, 315-325.
34. Staeva-Vieira, E. (2003). Maternal-effect Screen Identifies Genes Necessary For DSB Repair and Oocyte Development. In *Cell Biology*. (New York: New York University Medical Center).

Curriculum Vitae

[Redacted]

[Redacted]

[Redacted]

[Redacted]

[Redacted]

[Redacted]

[Redacted]

[Redacted]

[Redacted]

[Redacted]

[Redacted]

[Redacted]

[Redacted]

[Redacted]

[Redacted]

[Redacted]

[Redacted]

[Redacted]

[Redacted]

[Redacted]

[Redacted]

[Redacted]

[Redacted]

[Redacted]

[Redacted]

[Redacted]

[Redacted]

[Redacted]

[Redacted]

[Redacted]

[REDACTED]

[REDACTED]

[REDACTED]

[REDACTED]

[REDACTED]

[REDACTED]

[REDACTED]

[REDACTED]

[REDACTED]

[REDACTED]

[REDACTED]

[REDACTED]

[REDACTED]

[REDACTED]

[REDACTED]

[REDACTED]

[REDACTED]

[REDACTED]

[REDACTED]

[REDACTED]

[REDACTED]

[REDACTED]